IEEE Access
Multidisciplinary | Rapid Review | Open Access Journal

Received January 30, 2020, accepted February 27, 2020, date of publication March 5, 2020, date of current version March 13, 2020.

Digital Object Identifier 10.1109/ACCESS.2020.2978582

An Adaptive on-Demand Multipath Routing Protocol With QoS Support for High-Speed MANET

ZHENG CHEN, WENLI ZHOU, (Member, IEEE), SHUO WU, AND LI CHENG
School of Optical and Electronic Information, Huazhong University of Science and Technology, Wuhan 430074, China
Corresponding author: Wenli Zhou (wlzhou@hust.edu.cn)

ABSTRACT The mobility and resource limitation of nodes are the critical factors that affect the performance of Mobile AD hoc network (MANET). The mobility of nodes will affect the stability of links, and the limitation of node resources will lead to congestion, so it is very difficult to design a routing protocol that supports quality of service (QoS) in MANET. Especially in the scenario of high-speed node movement, frequent link interruption will damages QoS performance, so it is necessary to design MANET routing protocol that can adapt to network topology changes to support QoS. In this paper, we propose a Topological change Adaptive Ad hoc On-demand Multipath Distance Vector (TA-AOMDV) routing protocol, which can adapt to high-speed node movement to support QoS. In this protocol, a stable path selection algorithm is designed, which not only takes node resources (residual energy, available bandwidth and queue length) as the path selection parameters, but also considers the link stability probability between nodes. Furthermore, in order to adapt to the rapid change of topology, link interrupt prediction mechanism is integrated into the protocol, which updates the routing strategy based on periodic probabilistic estimates of link stability. Different scenarios with node speed in the range of 10-50m/s, data rate in the range of 4-40kbps and number of nodes in the range of 10-100 are simulated on NS2 platform. Our results show that the QoS metrics (packet delivery rate, end-to-end delay, and throughput) of the proposed protocol are significantly improved when the node speed is higher than 30m/s although it is slightly better when the node speed is lower than 30m/s. Our on-demand multipath routing protocol demonstrates high potential to support QoS for high-speed MANET.

INDEX TERMS Mobile ad hoc network, link stability, QoS, multipath routing, cross layer.

I. INTRODUCTION

MANETs has been widely applied in a great variety of scenarios, such as in disaster recovery, video conferencing and health care, battlefield communications, where audio/video data are most likely to be transmitted [1]. With the development of IoT, smart devices as network nodes are further promoting the applications of Mobile ad hoc network (MANET)[2]. However, the huge demand of multimedia transmission services require the provision of a quality of service (QoS)[3]. Nowadays, it is very challenging to guarantee QoS in MANETs because they not only lack satisfactory management and scheduling of resources by central node, but also suffer from external interference and internal failure such as link failure, battery failure, burst traffic, heavy traffic, and process failures [4]. Firstly, the mobility of the nodes changes the network topology in an unpredictable manner, which in turn affects the stability of links [5]. Secondly, the mobile nodes are typically battery constrained and the battery failure of a node affects not only that particular link but also the whole network topology [6]. Thirdly, it is needed to manage the network to meet the requirement of communication quality when resources (bandwidth, queue length, battery capacity, etc.) are limited [7]. These issues may not only increase latency and packet loss rate but also reduce throughput. Therefore, research and development on new routing technique in MANET adapting to the dynamic changes and resources constrained are highly desirable [8]–[11].

Traditional single-path routing algorithms such as Ad hoc On-demand Distance Vector (AODV) and Dynamic Source Routing (DSR) find the shortest path to the destination in MANETs with limited node resources. But, the shortest path is not always the optimal and stable path if there is a node with insufficient resources or excessive load, QoS performance

The associate editor coordinating the review of this manuscript and approving it for publication was Huan Zhou.

will be affected due to traffic congestion at that node. Therefore, some routing protocols add other parameters of the node like the available bandwidth, remaining energy and link stability into the algorithms of path selection. For example, a QOSAODV protocol that considers available bandwidth and link stability, an Energy and QoS supported AODV (EQ-AODV) taking into account the residual energy of the sensor and the type of packet to be sent when selecting the routing path appeared [12].

Multipath routing with alternate paths provides more reliable network services in network with dynamic topology changes. With backup path, multiple paths routing can quickly switch paths to restore data transmission after node failure and link failure. In addition, it can offer load balancing, better fault-tolerance, and higher aggregate bandwidth [13].

With the demand upgrading of QoS support, multipath routing protocols are kept improving for one decade. For example, taking into account the available resources of nodes, such as available bandwidth, idle queue length, battery level, etc [14], multipath routing protocol can compare the available resources of node in different paths and select the optimal path to transmit data to support QoS. Nowadays, path selection parameters in MANET include not only the available resources of nodes on the path, but also the path stability. Researchers are seeking for various factors to effectively evaluate the path stability. However, so far, in the scenario of high-speed movement of resource-limited nodes, the routing protocol of adaptive link state changing rapidly to support QoS has not been intensively investigated yet. It is also more challenging to find appropriate criteria for path stability.

The main objective of this study was to improve QoS performance in high-speed MANET by designing an adaptive topological changes on-demand routing protocol. In this routing protocol, a stable path selection algorithm is designed to reduce the delay of path switching, and a monitoring mechanism of link interruption probability is designed to reduce packet loss due to link interruption. The proposed protocol might be used as an effective solution for high-speed MANET with QoS requirements and resource constraints, such as vehicle-to-vehicle multimedia communication, mobile video monitoring network, etc.

The rest of the paper is organized as follows: Section 2 discusses the QoS performance of several routing protocols applied to MANET at different speeds; Section 3 mainly describes the stable path selection algorithm and link stability monitoring mechanism in our proposed Topological change Adaptive Ad hoc On-demand Multipath Distance Vector (TA-AOMDV) routing protocol; The results and evaluation of the proposed routing protocol are presented in section 4. Finally, Section 5 concludes the study and presents future work.

II. RELATED WORK

This section mainly reviews some multipath routing protocols to cope with network topology changes and discusses their QoS performance.

Ad hoc On-demand Multipath Distance Vector (AOMDV) [15] routing protocol can provide partial QoS guarantee as it switches to the alternative path to continue communication when the path is interrupted. In order to better support QoS, Chen *et al.* proposed QoS-AOMDV routing protocol in [14]. This protocol obtains the information of residual energy and queue length by cross-layer, and combines these information to form a selection criterion for high-quality paths. In MANET, QoS performance of QoS-AOMDV will be degraded due to node mobility. Because the fast change of network topology will cause frequent path interruption, QoS-AOMDV has to switch paths frequently, which will eventually lead to QoS degradation. Therefore, path stability is considered when choosing alternative paths, e.g., some calculate the stability probability of the corresponding path based on the distance between nodes or the received signal strength.

Periyasamy *et al.* proposed a protocol called link reliable multipath routing (LRMR) [16]. It finds multiple link reliable paths between any source and destination pair using two metrics such as Path Length and Path-Link Quality Estimator (P-LQE). It also reduces the probability of routing interrupts in a dynamic Ad hoc network. However, the LRMR does not consider the resources of the node, such as residual energy and available bandwidth, so QoS can only be supported to a certain extent. The End-to-End Link Reliable Energy Efficient Multipath Routing (E2E-LREEMR) protocol uses P-LQE and Path-Node Energy Estimator to find multiple reliable energy saving paths between any source and destination pair for data transmission [17]. A path selection strategy based on energy constraint and link stability is proposed [18], mainly utilizing message delay between the sending and receiving time to measure link stability. Rump *et al.* present the Probabilistic Routing In Mobile Environments (PRIME) routing protocol [19], which uses a probabilistic multipath forwarding process to increase route stability in dense scenarios with high network load. In the process of neighbor discovery, topology information is obtained by receiving signal strength and periodically broadcast to other neighbor nodes. Aiming to the special needs of the medical wireless network, Liu *et al.* proposes a reliable multipath routing protocol (RRMP) with two path selection factors considered: link stability factor and time constraint value, providing low link interruption probability and delay [20]. Gomes *et al.* proposes a Link Quality Estimator (LQE) for industrial WSN, and the dedicated node in WSN estimates the link quality based on received signal strength [21]. Nevertheless, the estimation of link stability only by distance are not suitable for high-speed scenarios such as nodes moving at an average speed of 20m/s.

As the influence of node speed on QoS performance can be reflected by path lifetime. Path with longer lifetime can provide better QoS due to the stability of the transmission path for a long time. In [22], a cross-layer approach to build durable and robust routing is proposed for the scenario of uniform node motion. This is done by considering the distance between two vehicles to estimate Link Residual Time (LRT).

This route can maintain a high quality of service when the node speed range is 4-20 m/s. In reality, the uniform motion of nodes is very rare, and the stability of the path cannot be accurately described by only referring to the distance factor. Therefore, some routing algorithms, including Optimized Link State Routing Protocol (QOLSR) and Energy Efficient and Stable Multipath Routing (EESMR) [23], [24], taking into account other factors, such as node speed and node available resources. The two routing protocols were within the speed range of 0.8-8 (m/s) and 2-10 (m/s) respectively, and some improvements in routing performance indexes such as packet delivery rate, end-to-end delay, throughput, energy efficiency and control overhead were verified. Some solutions introduced GPS modules to obtain more accurate path lifetime by more accurate distance between nodes and node speed. Wang *et al.* proposed the Passive Clustering Aided Routing protocol (PassCAR) for Vehicular ad hoc networks (VANETs) assuming that all nodes (speed range 22-33 m/s) are synchronized using a GPS clock [25]. The nodes with greater LLT values are selected as the CLUSTER_HEAD or GATEWAY node, achieving better path discovery, network throughput, and path lifetime than the original passive clustering mechanism. However, the GPS module in the node increases the economic cost and energy consumption, which has to be considered for resource-constrained MANET.

In resource-constrained MANET, the path selection algorithm make tradeoff between efficient resource allocation and path stability. The cost function integrating path stability and resource efficiency are introduced to evaluate the QoS performance that the path can provide. Through the path selection algorithm, the source node calculates the cost value of all alternative paths and selects the path with lower cost value to send data. For example, Gawas *et al.* proposed the QoS aware weight based on demand Multipath Routing protocol (QMR) in [26], which takes the received signal strength, residual energy and available bandwidth as parameters of the cost function. However, the QMR is not suitable for high-speed scenarios because the path selection metric does not consider the timeliness of link quality. In [27], the QoS is enhanced by a Cross-layer Multicast Routing (CLMR) through a tree-based multicast routing protocol. It exploits information of battery life, bandwidth from the physical layer, link stability factor from the routing layer and overhead of updating the tree from the application layer, and finally calculates the cost function based on the parameters of each layer. CLMR selects nodes with low cost to build stable routing paths. In [28], Singal *et al.* proposed a multi-constraints link stable multicast routing protocol by introducing a QoS metric called Link Stability cost Function (LSF) which is a multi-objective cost function constructed from contention count (CC), hop count and signal strength (distance), proven to be more efficient in terms of increased packet delivery ratio, reduced end-to-end delay for node moving speed in the range of 5-30m/s.

These routing protocol algorithms based on lifetime and cost functions can improve the QoS of high-speed MANET to some extent. However, in scenarios with higher speeds (greater than 30m/s), these routing algorithms become inefficient because path stability is difficult to dynamically represent with non-real-time path life and cost functions. At present, the methods that can adapt to the drastic change of network topology mainly include learning algorithm and periodical detection package mechanism.

In [29], Abbas and Fan proposed a new clustering-based reliable low-latency multipath routing (CRLLR) scheme by employing Ant Colony Optimization (ACO) technique for vehicular communication. In the relative velocity range of 5.5-27.7m/s, compared with the existing scheme, this routing scheme has better QoS index but higher energy consumption due to clustering and ACO technology. Lobiyal *et al.* proposed an algorithm based on Particle Swarm Optimization (PSO) to find an optimal path combination in AOMDV in real scenario [30]. The experimental results in the scenario with a speed of 15m/s show that the optimal combination of parameter values can reduce the average end-to-end delay by 80.65%, reduce the network routing load by 37.07%, and slightly reduce the packet delivery rate (1.96%). In [31], Giri *et al.* have used Teaching-Learning Based Optimization (TLBO) technique to find optimal value of parameters for AOMDV in given real scenario. When the speed is 15m/s, the optimal parameter value obtained by TLBO is used as the routing discovery parameter to significantly improve the average End-to-End delay (90.50% drop), the network routing load (41.68% drop) and the packet delivery ratio (0.39% rise) using value of parameters obtained through TLBO. However, learning algorithms generally requires a long learning time and a large amount of computation, so it is not suitable for MANET with fast topological change and limited node computing power.

A periodic packet detection can be used to monitor the real-time change of link state. For example, Naushad *et al.* proposed a novel Link Connectivity Metrics (LCM) and Path Distribution Analysis (PDA) strategies using Hello messaging in MANETs for path stability estimation among neighboring nodes inside a cluster [32]. In [5], Jabbar *et al.* Proposed MBMA-OLSR routing scheme in this paper extends and enhances the conventional MP-OLSRv2 routing protocol. Control messages (HELLO and TC) gather all the network topology information to construct the network graph. Through network graph, MBMA-OLSA can avoid nodes with higher speeds and lower residual battery power, and choose more stable links. MBMA-OLSR is significantly superior to MP-OLSRv2 in throughput, end-to-end latency, and packet delivery rates in the range of 5-30m/s. The control cost of routing protocol and occupies the channel bandwidth was increased by using periodic packet detection method even though the adaptability of topology changed was improved.

To sum up, it is very challenging to design a routing protocol with resource constraint and QoS guarantee for high-speed MANET. In this paper, we propose a multipath routing protocol that can adapt to rapid topology

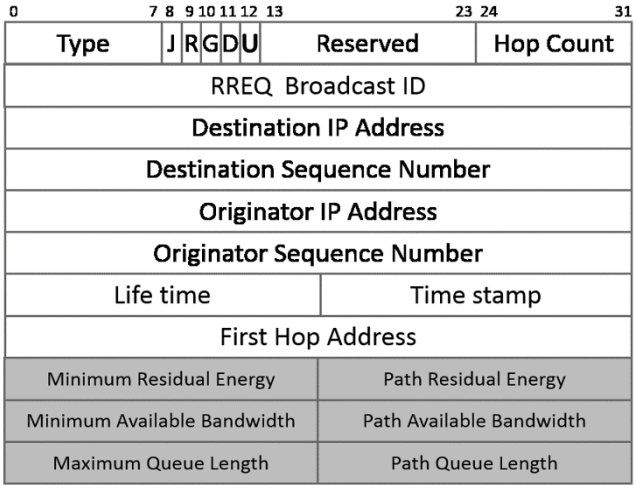

FIGURE 1. Format of New RREQ packet.

change and try to guarantee QoS in MANET. Simulation and performance analysis of our proposed TA-AOMDV routing protocol are conducted in comparison with AOMDV, LRMR, QoS-AOMDV and QMR routing protocol, using the NS-2.35 simulator.

III. THE PROPOSED TA-AOMDV

The main purpose of our TA-AOMDV is to provide communication services that can guarantee certain QoS in high-speed scenes. TA-AOMDV first obtains several alternative paths with better QoS performance by the alternative path selection algorithm, and then the primary path selection algorithm selects the most stable path from the alternative path to transmit data. Finally, the link interruption probability prediction mechanism enables TA-AOMDV to adapt to the drastic topological changes caused by the high-speed movement of nodes. The following details describe the design of the routing protocol and the implementation of the algorithm.

A. TA-AOMDV PROTOCOL DESIGN

1) ROUTE DISCOVERY PROCESS

The main task of TA-AOMDV routing discovery is to find all routing paths with sufficient communication resources. In this process, an alternative path selection algorithm is executed at the destination node, which can obtain the desired path according to the information of related resources provided by the intermediate node. Specific process analysis is as follows.

At the beginning of route discovery, the source node generates the RREQ packet, which is formatted as shown in Fig. 1. Compared with RREQ format of AOMDV, the format in the figure adds new fields to store energy, bandwidth, and queue length information.

When an intermediate node receives a RREQ, TA-AOMDV need to update the energy, bandwidth, and queue length values in the RREQ field, and then broadcast the new RREQ to its one-hop neighbor. The processing of RREQ by the intermediate node is shown in Fig. 2.

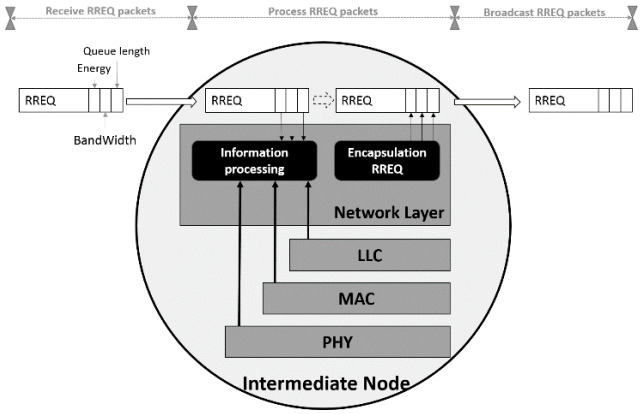

FIGURE 2. The Intermediate nodes process and forward RREQ. After the intermediate node receives RREQ, the information processing module of the network layer extracts the energy, bandwidth and idle queue length information in the RREQ field. The second step is to obtain energy information at the physical layer, bandwidth at the MAC layer and idle queue length at LLC through the cross-layer interface. The third step is to calculate the minimum value and average value of the two groups of information respectively, and broadcast RREQ after updating the field of RREQ.

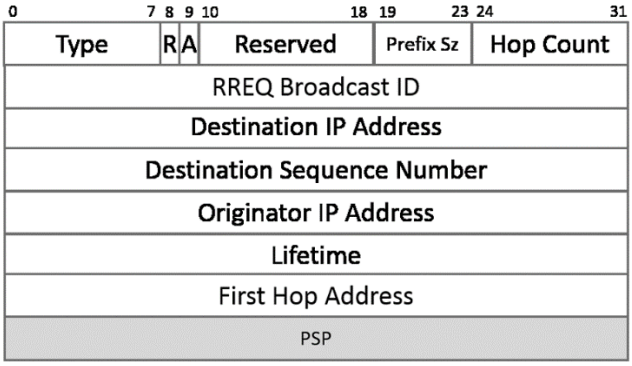

FIGURE 3. Format of New RREP packet.

The destination node starts the timer immediately after receiving the first RREQ. After the timer ends, the alternative path selection algorithm extracts the RREQ information to calculate the cost function of the path.

2) ROUTE REPLY PROCESS

In the routing reply process, each intermediate node calculates the stable probability of the path that the RREP packet travels through, and the whole process terminates at the source node. The packet format for RREP is shown in Fig. 3. Compared with AOMDV, the packet format of TA-AOMDV adds the field of Path Stability Probability (PSP).

After the source node obtains the stable probability of the path, the primary path selection algorithm will arrange all alternative paths in descending order according to the stable probability of the path, and select the first path as the path for data transmission.

3) ROUTE MAINTENANCE PROCESS

In order to reduce packet loss and retransmission caused by link interruption, a topology change monitoring and feedback

mechanism is embedded in routing maintenance. In this mechanism, the node on the path monitors the probability of link stability with the next-hop node and sends a Link Abnormal Status Notification (LASN) packet to the source node when the probability falls below the threshold. The LASN sent by the node contains the ID number of the corresponding node that makes up the unstable link.

When an intermediate node receives RREQ, RREP, and LASN, the routing update rule of TA-AOMDV is invoked to update the routing table. After the intermediate node receives the RREQ, it will add the route entry (to the source node) in the reverse route table and re-broadcast the RREQ. When the node receives the RREP, it will add the route entry (to the destination node) to the forward route table and look for the reverse route to send the RREP. If the intermediate node receives LASN, it deletes the route entry connected to the unstable link and looks for the reverse route to continue sending LASN.

B. ALTERNATIVE PATH SELECTION ALGORITHM

The destination node starts the timer immediately after receiving the first RREQ. After the timer ends, the alternative path selection algorithm extracts RREQ information to calculate the cost function of the path. These information will be used as the conditional parameters of alternative path selection, specifically described as follows:

- Energy metric
  In order to achieve high energy efficiency, the routing algorithm must consider the energy factor when choosing alternative paths. In RREQ packet, two fields are added to store the average residual energy and the minimum residual energy respectively. The calculation of the average residual energy is as follows:

$$\overline{E_{path}^{residual}} = \frac{1}{N}\sum_{i=1}^{N} E_i^{residual} \tag{1}$$

  The minimum residual energy is calculated as follows:

$$E_{min}^{residual} = \min_{1\le i\le N} E_i^{residual} \tag{2}$$

  where N represents the number of hops saved in RREQ and $E_i^{residual}$ represent the residual energy of a node.
- Bandwidth metric
  In order to calculate the channel utilization, the busy and idle states of the channel need to be detected periodically. Eq. (3) is the mathematical model of channel state detection.

$$u_i(t = \begin{cases} 0 & H_0(idle) \\ 1 & H_1(busy) \end{cases} \tag{3}$$

  The channel utilization (Eq. (4)) and available bandwidth (Eq. (5)) of node i are estimated as follows:

$$U_i\,(t, t + M\tau) = \frac{1}{M}\sum_{m=1}^{M} u_i(t + m\tau) \tag{4}$$

$$B_i\,(t, t + M\tau) = B_{channel}^{gross}\,[1 - U_i(t, t + M\tau)] \tag{5}$$

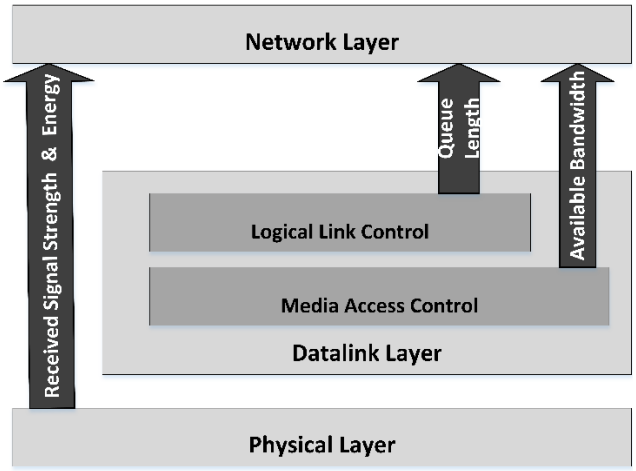

FIGURE 4. Cross-layer network architecture. An interface is established in the physical layer through which the network layer can obtain node residual energy and received signal strength information. The same interfaces are created at LLC and MAC in the data link layer, therefore the network layer gets queue length and available bandwidth information from the interface, respectively.

where M represents the number of samples, τ represents the sampling interval, and $B_{channel}^{gross}$ represents the channel gross bandwidth.
Further, the average bandwidth (Eq. (6)) and minimum bandwidth (Eq. (7)) can be calculated respectively from available bandwidth.

$$\overline{B_{path}} = \frac{1}{N}\sum_{i=1}^{N} B_i \tag{6}$$

$$B_{min} = \min_{1\le i\le N} B_i \tag{7}$$

- Queue length metric
  Idle queue length of node can be calculated by formula (8), as follows:

$$QL_i^{idle} = QL_i^{initial} - QL_i^{occupied} \tag{8}$$

Equations (9) and (10) respectively calculate the minimum queue length value and the average queue length value, which are encapsulated in RREQ.

$$QL_{min}^{idle} = \min_{1\le i\le N} QL_i^{idle} \tag{9}$$

$$\overline{QL_{path}^{idle}} = \frac{1}{N}\sum_{i=1}^{N} QL_i^{idle} \tag{10}$$

However, the remaining energy information, available bandwidth information and queue length information come from the physical layer, MAC layer and LL layer respectively. Therefore, for MANET adopting traditional layer method, it is difficult to obtain information of other layers in the network layer [27]. As shown in Fig. 4, the TA-AOMDV utilizes a cross-layer network architecture to obtain energy information, queue length, available bandwidth and received signal strength at the network layer. During the routing request, the cross-layer information including node energy,

queue length, and available bandwidth are encapsulated in RREQ and sent to the destination node.

After the destination node receives RREQ, the cost function of the three factors are calculated by Eq. (11), Eq. (12), and Eq. (13) respectively.

$$C_j^{energy} = \frac{\overline{E_{path}^{residual}}}{E_{min}^{residual}} \tag{11}$$

$$C_j^{bandwidth} = \frac{\overline{B_{path}}}{B_{min}} \tag{12}$$

$$C_j^{QL} = \frac{\overline{QL_{path}^{idle}}}{QL_{min}^{idle}} \tag{13}$$

The cost function of the path can be obtained as follows:

$$C_j = \alpha \cdot C_j^{energy} + \beta \cdot C_j^{bandwidth} + \gamma \cdot C_j^{QL} \tag{14}$$

Here, $\alpha + \beta + \gamma = 1$, the values of α, β, and γ reflects different networks features. Different values of α, β, and γ can be selected depending on the performance of the network. To focus on the different path energies, the values of the three weight coefficients are as follows:

$$\begin{cases} \alpha = 1 - \frac{\overline{E_j^{residual}}}{E_j^{initial}} \\ \beta = \frac{1-\alpha}{2} \cdot \frac{\overline{B_j}}{B_{channel}^{gross}} \\ \gamma = \frac{1-\alpha}{2} \cdot \frac{\overline{QL_j^{idle}}}{QL_j^{initial}} \end{cases} \tag{15}$$

The destination node calculates the cost function value of each RREQ and selects three paths with the lowest cost value as the alternative path. The destination node sends the RREP to the source node in turn along the alternative path.

C. PRIMARY PATH SELECTION ALGORITHM

The primary path selection algorithm of source node can choose the most stable path among alternative paths to transmit data. In order to obtain the Path Stability Probability (PSP), the source node must obtain the stability probability of each link forming the path firstly. The intermediate node estimates the link stability probability (LBP) through the signal strength of the received RREP, and updates the PSP field of the RREP, and finally transfers it to the source node. The estimates of LBP and PSP are as follows:

- Link Break Probability (LBP)
  It is difficult to predict when the link will break in MANET. But we can estimate the relative stability of the link, by comparing the recent and current signal strengths. The signal strength varies with the distance, so the distance is a good metric to measure the reliability of link.
  For the sake of simplicity, some assumptions must be done to obtain an analytical model. We assume that the node movement model is a Random Waypoint Mobility Model (RWMM), and all nodes move in a rectangular region with the same movement parameters. The initial positions of all nodes are uniformly distributed within the rectangular region. The probability distribution function (pdf) of the distance between two nodes obeys normal distribution, and its cumulative distribution function is as follows:

$$CDF_d(r) = P_{(d \le r)} \cong \frac{r}{R}, 0 \le \mathrm{r} \le \mathrm{R} \tag{16}$$

In the RWMM, the probability density function of the distance between two nodes exceeding the transmission range is shown in equation (16).

$$pdf_{2node}(r) = \frac{4}{\pi R^2} \cdot \sqrt{R^2 - r^2}, 0 \le \mathrm{r} \le \mathrm{R} \tag{17}$$

$$\begin{aligned} LBP_{(r,R)} &= \int_0^r P_{(d>r)} \cdot pdf_{2node}(r) \cdot dr \\ &= \int_0^r (1 - CDF_d(r)) \cdot pdf_{2node}(r) \cdot dr \\ &\approx \int_0^r \left(1 - \frac{r}{R}\right) \cdot \frac{4}{\pi R^2} \cdot \sqrt{R^2 - r^2} \cdot dr, \end{aligned} \tag{18}$$

In order to reduce computational overhead, equation (18) is further simplified to equation (19) [13].

$$LBP_{(r,R)} \approx 1 - e^{-\frac{r}{R}}, 0 \le \mathrm{r} \le \mathrm{R} \tag{19}$$

Although the simplified formula will bring an average relative error of 9.5%, there is a good trade-off between computational complexity and accuracy. Moreover, the simplified LBP expression can easily estimate Path Break Probability.

- Path Stability Probability (PSP)
  When node receives RREP from the destination node, PSP value in RREP is extracted, and LBP value of link between two nodes is calculated by using equation (19). Equation (20) can be used to calculate the new PSP value and update the PSP field in RREP. Finally, Path Interruption Probability (PIP) value of path can be calculated at the source node through equation (21), which can be used to select the most stable path among alternative paths.

$$PSP_j = \prod_{l=1}^{L} (1 - LBP_l) \tag{20}$$

$$PIP_j = 1 - PSP_j \tag{21}$$

The path list is updated when the source node receives RREP. After obtaining the PSP value from the RREP, the primary path selection algorithm selects the path with the minimum PIP value as the primary path for data transmission.

Fig. 5 shows the route selection process of the TA-AOMDV protocol. The RREQ sent by the source node can obtain the resource information of the intermediate node that is passed through. After receiving the RREQ, the destination node calculates the cost value through the cost function to determine the available path. Next, the destination node selects the low cost of the available paths as the alternative path and sends the RREP on those alternative paths. Finally, the primary path is selected after the source node receives the RREP containing the path interrupt probability (PIP).

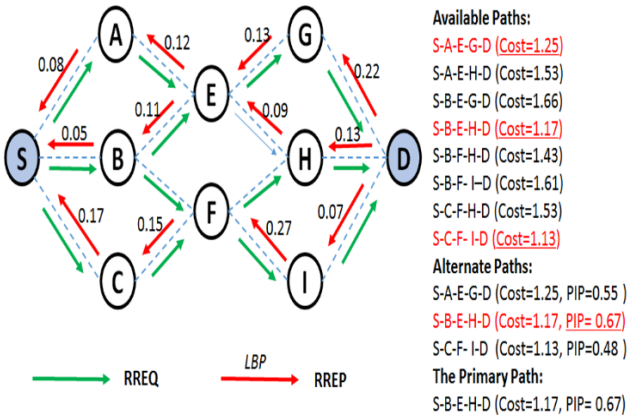

FIGURE 5. Route Selection Process of TA-AOMDV protocol. The source and destination nodes are represented as S and D, respectively. The green arrow represents the path of the RREQ packet. RREQ contains information to calculate the cost values (residual energy, available bandwidth, and queue length). The red arrow represents the RREP, and the number represents the link break probability.

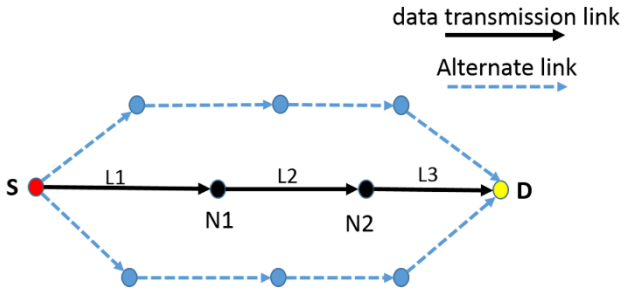

FIGURE 6. Node monitoring link diagram. In order to reduce the calculation cost of link stability probability, the node only monitors the link formed by the next hop node in the routing table. For example, node N1 monitors the link L2 formed with the next-hop node (N2).

D. TOPOLOGY CHANGE MONITORING AND FEEDBACK MECHANISM

1) LINK INTERRUPTION PROBABILITY MONITORING

The interruption probability of a link belonging to an established path is monitored by the strength of the received signal from next hop node on real time. When the link interruption probability exceeds the threshold, the source node is notified and switched to an alternate path to continue communication. To avoid increasing network traffic load, the mechanism uses periodic HELLO packets to sense link stability.

As shown in Fig. 6, Links L1, L2 and L3 form the primary path, and there are two alternative paths. In the primary path, node S monitors link L1, node N1 monitors link L2, and node N2 monitors link L3. For example, after node N1 receives the HELLO packet from the neighbor node, it first looks up the address of the next-hop node in the routing table. If it is the HELLO packet from node N2, the stability of link L2 is calculated through the received signal strength. If N1 estimates that L2 will be interrupted, N1 will send Link Abnormal Status Notification (LASN) packet to the source node. After receiving LASN packet, the source node searches the path list. If there are alternate paths in the list, it will switch paths, otherwise reroute.

In addition, the monitoring mechanism of the two alternative paths in Fig. 6 is the same as the primary path. If the source node receives the LASN package sent by the node in the alternative path, the source node deletes the alternative path from the path list.

2) LINK INTERRUPTION PROBABILITY ESTIMATION

In the process of link interruption probability monitoring, the relative distance between nodes is used to estimate whether the link will be interrupted. The relative distance between nodes is calculated from the received signal strength of the HELLO packet. To reduce the computational overhead, the node does not need to calculate the relative distance of all neighbor nodes, but only the distance from the next hop node.

Each time the HELLO packet is received, the node calculates the distance according to the received signal strength. From equation (22), the average velocity can be obtained by the distance variation in the time interval.

$$v_n = \frac{\Delta r}{\Delta t} = \frac{r_n - r_{n-1}}{\Delta t} \tag{22}$$

Here, v_n represents the instantaneous rate at time n $\cdot$ Δt, r_n represents the distance measured this time, r_{n-1} represents the distance measured last time, and Δt represents the time interval received from HELLO packet.

Since the rate is a continuously changing analog quantity, the time interval of the HELLO packet is less than 1 second. Therefore, as shown in the equation, the instantaneous rate at time (n+1) * Δt can be approximated.

$$v_{n+1} \approx v_n \tag{23}$$

$$r_{n+1} = v_{n+1} \cdot t + r_n \approx v_n \cdot t + r_n \tag{24}$$

If the value of r_{n+1} is greater than the communication range, the node immediately sends the LASN packet to the source node.

IV. SIMULATION AND EVALUATION

A. SIMULATION ENVIRONMENT

In order to evaluate the performance of the proposed routing protocol at different node speeds, different node densities, and different traffic loads, three different scenarios are established. Specific simulation parameters are shown in Table 1.

In the first scenario, we study the performance of the protocol at different node speeds. We set 30 nodes randomly distributed in a 1000 m$\times$1000 m area, and pre-defined CBR data rate of 16 Kbps. The range of node movement speed is 10-50m/s, and the experimental simulation time is 120 seconds. The node starts moving and sending data after an initial 10 seconds.

In the second scenario, the protocol behavior under different CBR data rate is studied. The number and speed of nodes were set at 30 and 10 m/s, respectively.

In the last scenario, we vary the number of nodes participating in the network from 10 to 100 randomly distributed

TABLE 1. Simulation parameters.

Parameter	Value	Unit
Number of nodes	10, 20, 30… 100	node
Node speed	0, 10, 20, 30, 40, 50	m/s
Simulation area	1000*1000	m^2
Queue length	50	packet
Routing protocol	TA-AOMDV, QMR, LRMR, QOS-AOMDV, AOMDV	
MAC layer	IEEE 802.11	
CBR Packet size	512	bytes
CBR data rate	4, 8, 12, 16… 40	Kbps
Transmission range	250	m
Mobility model	Random way point	
Channel bandwidth	2	Mbps
Carrier frequency	2.4	GHz
Initial energy	100	Joules
Transmission power	0.66	Joules
Received power	0.395	Joules
Simulation time	120	s

in an area of 1000 m × 1000 m. We set the constant node velocity of 10m/s and CBR data rate of 16Kbps.

B. PERFORMANCE METRICS

In order to evaluate the QoS support of the proposed routing protocol, the main performance metrics used in the simulation experiment are packet delivery rate (PDR), end-to-end delay (E2ED), throughput. In addition, because the LASN package is introduced into the route maintenance process, it is necessary to investigate the route control overhead, that is, Routing Overhead Ratio (ROR). The details of these metrics are described below:

- ***Packet Delivery Rate (PDR):*** The ratio of the number of packets received by the target node to the number of packets actually sent by the source node is called PDR. The calculation formula is as follows:

$$PDR = \frac{\sum_{i=0}^{n} R_i^{pkt}}{\sum_{j=0}^{m} S_j^{pkt}} \tag{25}$$

  Here R_i^{pkt} represents the number of packets received, and S_j^{pkt} represents the number of packets sent.
- ***End-to-End delay (E2ED):*** E2ED is the average time for a packet successfully transmit a message from the source to the destination across the network. E2ED is calculated thusly:

$$E2ED = \frac{\sum_{i=0}^{n} (t_i^{received} - t_i^{send})}{n} \tag{26}$$

  In this equation, n represents the number of successfully received packets; $t_i^{received}$ represents the current time the destination node received the *i*th packet; t_i^{send} represents the current time the source node sent the *i*th packet.
- ***Throughput:*** Throughput refers to the number of bits received by the destination node during simulation time.

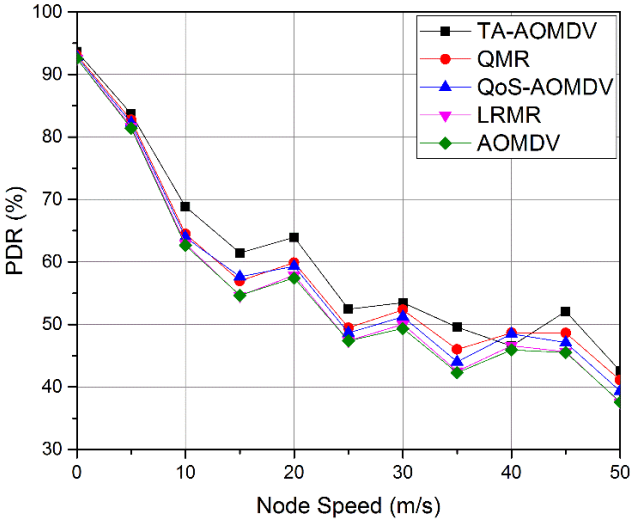

FIGURE 7. Packet delivery ratio against node speed.

Stated below is the formula to calculate the throughput:

$$Throughput = \frac{\sum_{i=0}^{n} R_i^{Byte}}{t^{sim}} \tag{27}$$

Here, R_i^{Byte} and t^{sim} represent the total number of bytes received by all nodes and the simulation duration, respectively.

- ***Normalized Routing Overhead (NRO):*** The normalized routing overhead is the ratio of the routing control packet to the number of packets received by the destination node. Routing control packets consume the available bandwidth and battery power of the nodes. Therefore, this metric represents the cost of control overhead for each data packet sent in the network. The following formula represents the computation of the routing overhead:

$$\text{NRO} = \frac{CP}{DP} * 100\% \tag{28}$$

  where CP and DP represent the total number of control packets and data packets, respectively.

C. SIMULATION RESULTS

1) PACKET DELIVERY RATE

Fig. 7 depicts the variation of the packet delivery ratio as a function of node's speed. When the node speed increases as (0, 10, 20, 30, 40, 50) m/s, the packet transmission rate of the three routing protocols tends to decrease. TA-AOMDV decreases from 93.24% to 43.49%, QMR decreases from 93.04% to 40.68%, QoS-AOMDV decreases from 93.09% to 39.24%, LRMR decreases from 92.45% to 37.53% and AOMDV decreases 92.5% to 37.6%. However, the TA-AOMDV always has higher packet delivery ratio than the other four routing protocols, especially in the scene of high-speed node movement. TA-AOMDV protocol has a high packet delivery rate, because the link interrupt prediction mechanism in the protocol can switch paths or reroute before

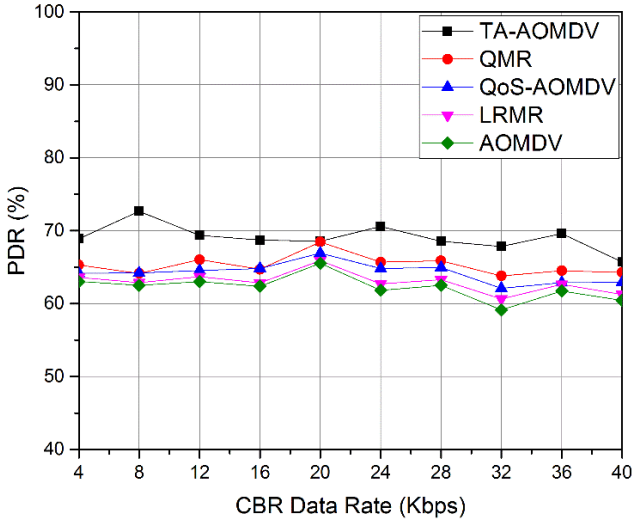

FIGURE 8. Packet delivery ratio against CBR data rate.

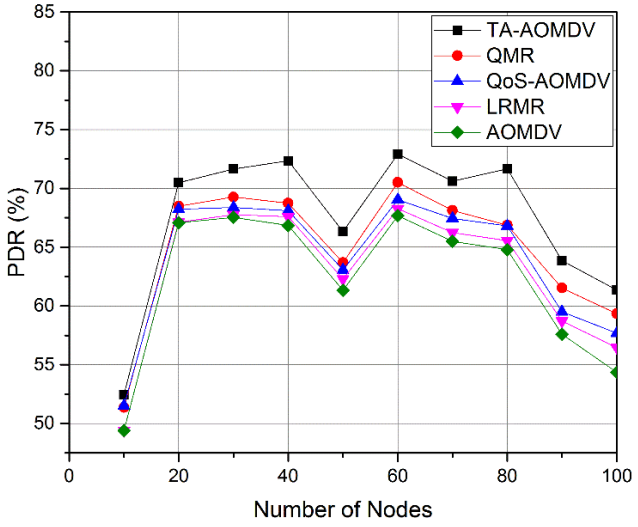

FIGURE 9. Packet delivery ratio against number of nodes.

the link interruption occurs, which reduces the number of packet retransmission.

Fig. 8 shows that CBR data rate changes have little impact on packet delivery ratio. With the change of the data rate, the performance metric of the three routing protocols all change little. The minimum value of TA-AOMDV is 64.17% and the maximum value is 71.34%. The packet delivery rates of QMR and QoS-AOMDV ranged from 64.21% to 72.07% and 62.08% to 67.66%, respectively. Obviously, the performance of the TA-AOMDV outperformed the other four routing protocols in terms of packet delivery ratio, as TA-AOMDV reduces the packet loss by selecting paths with higher QoS performance and periodically monitor path stability.

Fig. 9 shows the effect of different number of nodes on the packet delivery ratio. As shown in the figure, when the number of nodes is 10, TA-AOMDV, QMR, LRMR and

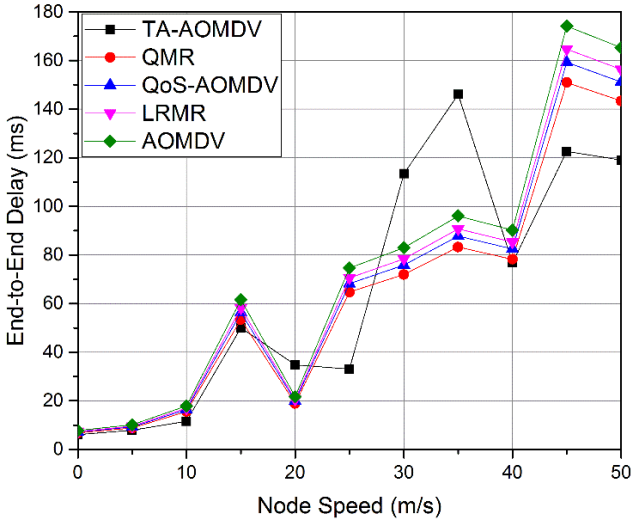

FIGURE 10. End-to-end delay against node speed.

QoS-AOMDV are 52%, 50%, 49.4% and 50.8% respectively. In the scenario where the number of nodes is 20, 30 and 40, as the number of nodes increases, a better quality path can be selected to transmit data, so the PDR of the four routing protocols (TA-AOMDV, QMR, LRMR and QoS-AOMDV) is improved, with the mean values of 72.7%, 70.8%, 67.5%and 68.4% respectively. When the number of nodes is set to 50, the packet delivery ratio decreases significantly. There are two reasons for the performance degradation: first, the traffic volume of data transmission increases with the increase of the number of nodes, which leads to the increase of path congestion probability; second, there are fewer alternative paths in multipath routing, and the quality of the paths is poor. But, after the number of nodes reaches 60, multiple paths of good quality can be selected, so PDR increases. After the number of nodes exceeds 60, the three routing protocols generally show a gradual decline trend due to path congestion.

2) END-TO-END DELAY

Fig. 10 depicts the performance of average end-to-end delay of packets against the node speed. When the node speed increases as (0, 5, 10, 15) m/s, the end-to-end delay increases. In the low speed scenario, the end-to-end delay indicators of the three routing protocols are very similar. When the node speed increases as (20, 25, 30, 35) m/s, the end-to-end delay also keeps increasing. In this speed range, the delay time of the proposed protocol increased sharply from 33.1ms to 146ms, and then decreased to 76.8ms after reaching 40m/s. The main reason for this phenomenon is the threshold setting of abnormal state feedback. If the node speed is in the range of 20-35m/s, the probability of triggering LASN packet transmission increases, and LASN packet transmission will cause the delay to increase. In high-speed scenarios(35, 40, 45, 50 m/s), frequent network topology changes lead to frequent interruption of alternate paths of multipath routing protocols, and failure of alternate paths will result in increased

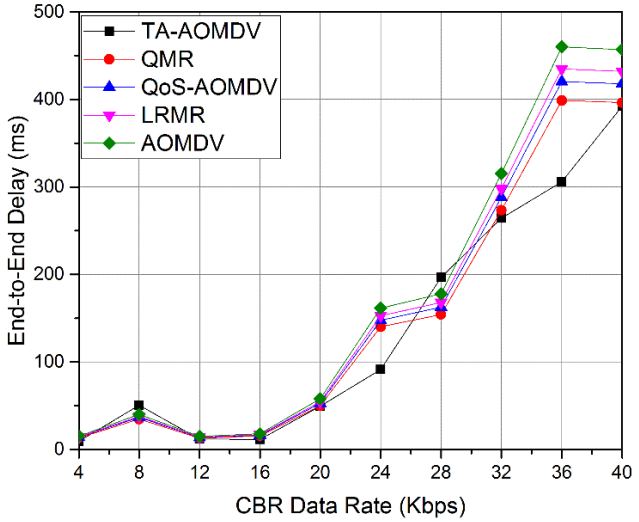

FIGURE 11. End-to-end delay against CBR data rate.

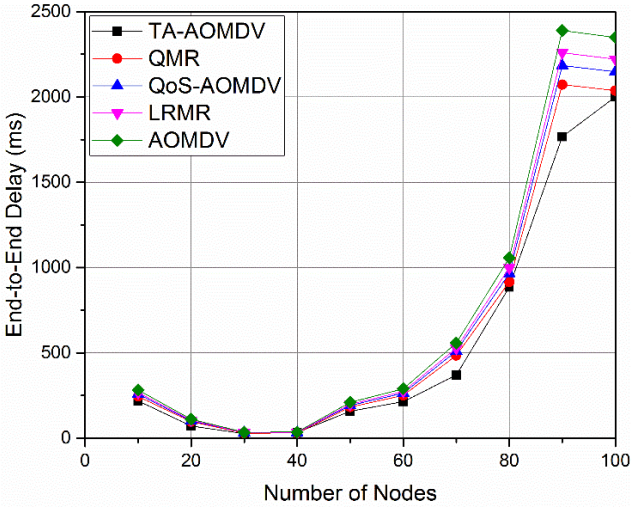

FIGURE 12. End-to-end delay against number of nodes.

end-to-end delay for rerouting or data retransmission. It is clear from the figure that TA-AOMDV has a lower end-to-end delay, especially when the speed is 50m/s, the delay of TA-AOMDV is only 71ms.

The main reason is that the stable path prediction mechanism in TA-AOMDV can monitor topological changes and switch the path or reroute before path interruption, which reduces the end-to-end delay caused by packet retransmission.

Fig. 11 shows the change of end-to-end delay at different CBR data rates. As the CBR data rate increases in the range of 4-40 Kbps, the end-to-end delay increases. The TA-AOMDV delay increases from 7.01ms to 398.89ms, the delay variation ranges of the four protocols (QMR, LRMR, QoS-AOMDV and AOMDV) are 9.67-459.73ms, 14.49-431.9ms, 13.65-407.01ms and 15.3-456.9 respectively. As shown in the figure, the end-to-end delay performance of the five routing protocols is very similar in scenarios with different CBR data rates.

Fig. 12 shows the end-to-end delay of three protocols in a scenario with different number of nodes. As the number of node increases in the 10-40 range, the end-to-end delay decreases. The TA-AOMDV routing protocol decreases from 251.99ms to 38.55ms. The reason for the reduced end-to-end delay is that the routing protocol can choose a better path to transfer data after the number of nodes increases. As the number of node increases in the 40-100 range, the end-to-end delay increases. In the scenario with different number of nodes, the end-to-end delay performance of TA-AOMDV protocol is slightly better than QMR, LRMR, QoS-AOMDV and AOMDV.

3) THROUGHPUT

Fig. 13 depicts the performance of average throughput of packets against the node speed. According to the throughput changes in the figure, the performance are

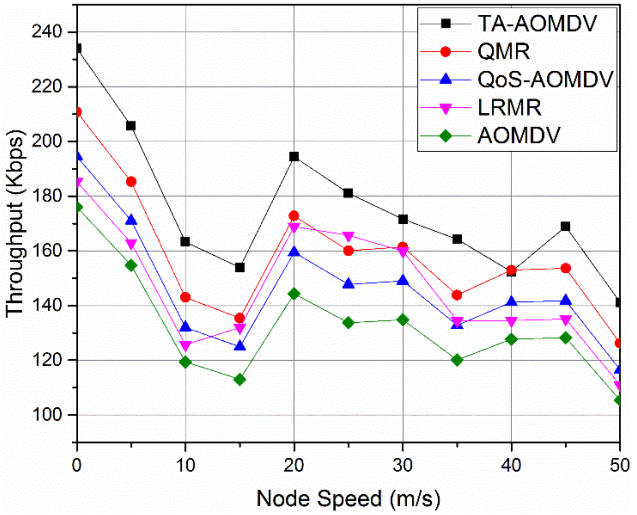

FIGURE 13. Throughput against node speed.

analyzed from two speed ranges. As the node speed increases (0, 5, 10, 15 m/s), the throughput of TA-AOMDV decreases from 233.60Kbps to 151.96Kbps. Within this speed range, TA-AOMDV has the best performance, followed by QMR, LRMR, QoS-AOMDV and AOMDV has the worst performance. When the node speed increases as (20, 25, 30, 35, 40) m/s, the throughput of TA-AOMDV decreases from 190.86Kbps to 145.72Kbps, QMR decreases from 178.24Kbps to 123.13Kbps, LRMR decreases from 168.9Kbps to 134.5Kbps, QoS-AOMDV decreases from 159.51Kbps to 116.50Kbps. Therefore, TA-AOMDV has the best performance in the range of 0-50m/s speed.

Fig. 14 shows the throughput changes in different CBR data rate scenarios. As the CBR data rate increases in the 4-40 Kbps range, the throughput of TA-AOMDV increases from 32.31Kbps to 456.86Kbps, TA-AOMDV has a more significant performance advantage compared with QMR, LRMR, QoS-AOMDV and AOMDV. In particular, when the

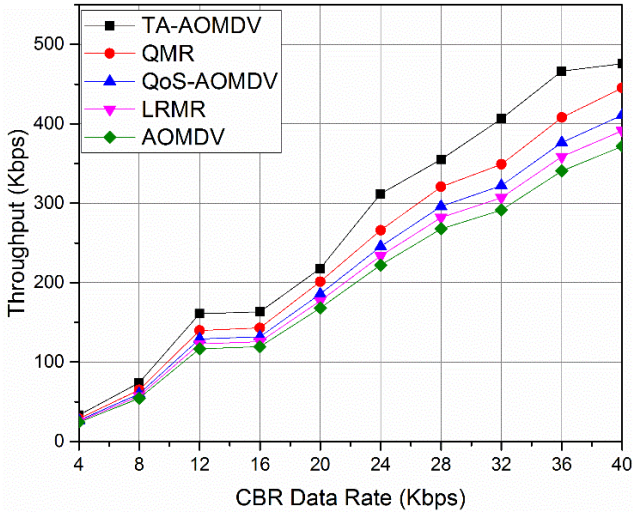

FIGURE 14. Throughput against CBR data rate.

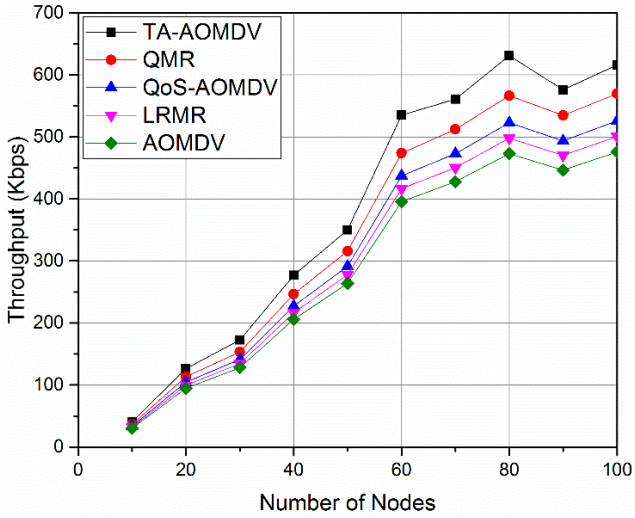

FIGURE 15. Throughput against number of nodes.

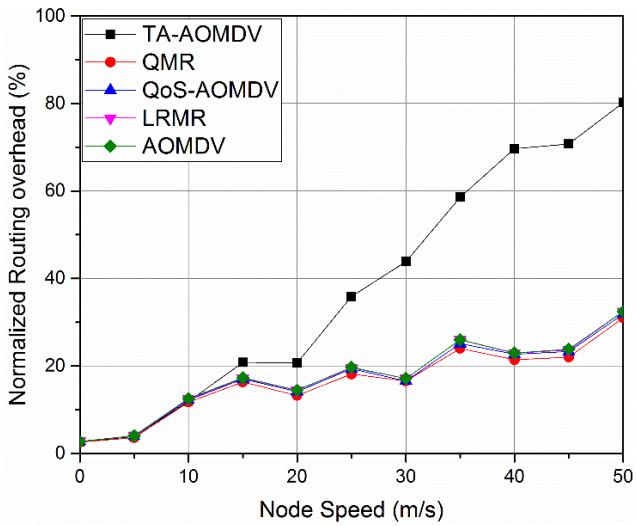

FIGURE 16. Normalized routing overhead against node speed.

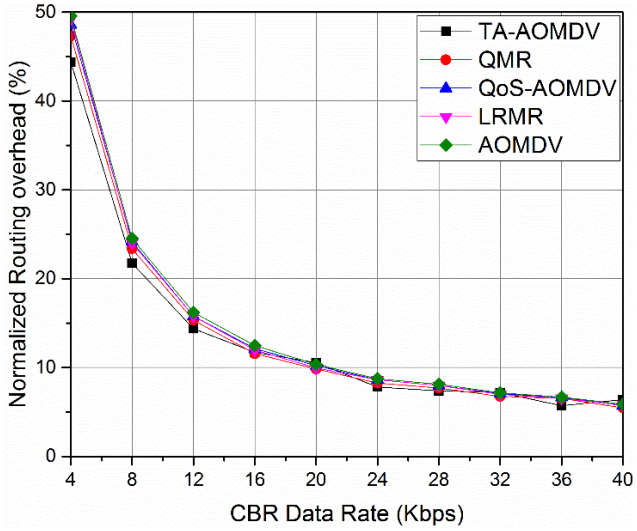

FIGURE 17. Normalized routing overhead ratio against CBR data rate.

CBR data rate is 36kbps, the throughput of TA-AOMDV is 14.36%, 30.1%, 23.9% and 36.9% higher than QMR, LRMR, QoS-AOMDV and AOMDV, respectively.

Fig. 15 shows the impact of different number of nodes on the throughput of TA-AOMDV, QMR, LRMR, QoS-AOMDV and AOMDV. As the number of nodes increases in the 10-100 range, the throughput of TA-AOMDV increases from 40.40Kbps to 662.38Kbps. As can be seen from the figure, as the number of nodes increases, TA-AOMDV has a more significant performance advantage compared with QMR, LRMR, QoS-AOMDV and AOMDV. In particular, when the number of nodes is 100, TA-AOMDV throughput is 16.1% higher than QMR and 25.9% higher than QoS-AOMDV, respectively. The main reason is that the number of nodes in the network increases so that TA-AOMDV, QMR and QoS-AOMDV easy to obtain more high-quality alternative paths.

4) NORMALIZED ROUTING OVERHEAD

Fig. 16 shows the effect of varying the node speed on the normalized routing overhead (NRO) for TA-AOMDV, QMR and QoS-AOMDV routing protocols. When the node speed increases as (0, 5, 10) m/s, the NRO increases as well. Due to the low node speed, the NRO of the five protocols is very close. When the node speed exceeds 10m/s, the NRO of TA-AOMDV increases even faster. In particular, when the node speeds is 50m/s, the NRO of TA-AOMDV is 49.2%, 47.8%, 48.4% and 46.9% higher than QMR, LRMR, QoS-AOMDV and AOMDV, respectively. The main reason is that the stable path prediction mechanism in TA-AOMDV sends a large number of LASN packets when the path is frequently interrupted.

Fig. 17 shows the NRO of TA-AOMDV, QMR, LRMR, QoS-AOMDV and AOMDV at different CBR data rates. As the CBR data rate increases in the 4-40 Kbps range, the NRO of TA-AOMDV decreases from 44.3% to 6.39%,

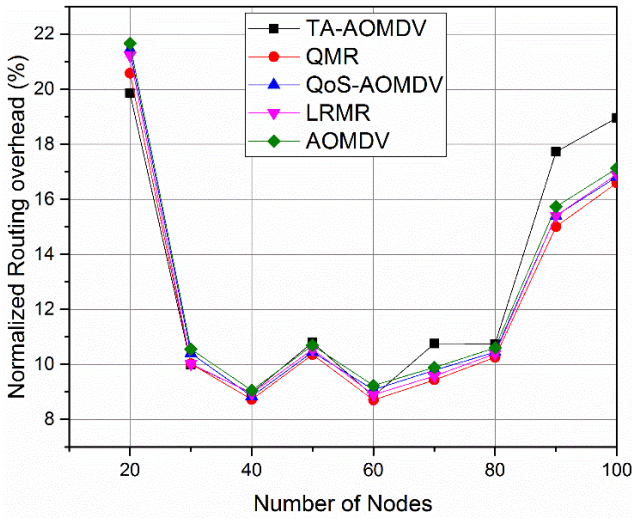

FIGURE 18. Normalized routing overhead ratio against number of nodes.

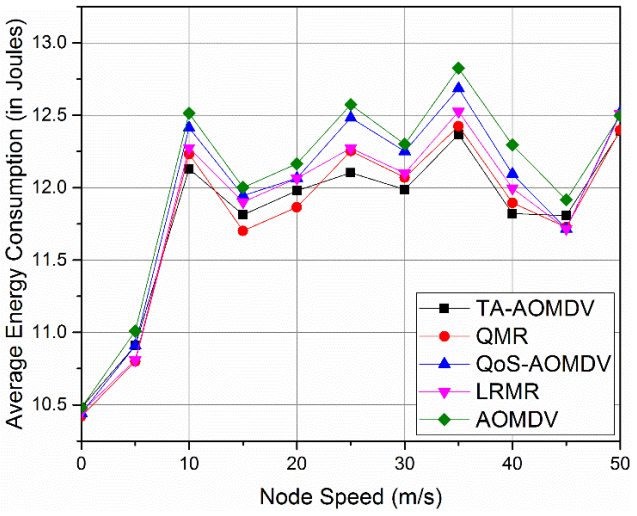

FIGURE 19. Average energy consumption against CBR data rate.

QMR decreases from 47.3% to 5.47%, LRMR decreases from 49.24% to 5.77%, QoS-AOMDV decreases from 48.59% to 5.71% and AOMDV decreases from 49.57% to 5.88%. In the scenario of different CBR data rates, the NRO of the three routing protocols is similar.

Fig. 18 shows the influence of different number of nodes on the NRO. As the number of nodes increases in the 10-40, the NRO of TA-AOMDV decreases from 47.69% to 7.81%, the routing overhead of the other four routing protocols also declined. The main reason for the decreasing routing overhead is that as the number of nodes increases, it is easier for the source node to find the path. As the number of nodes increases in the 40-100, the routing overhead of the five routing protocols is very close.

5) AVERAGE ENERGY CONSUMPTION

The average energy consumption here refers to the total energy consumed by all nodes after the destination node correctly receives a packet. This performance metric can well reflect the network energy efficiency.

Fig. 19 shows the average energy consumption (AEC) of the five routing protocols at different node speeds. Since TA-AOMDV, QMR and LRMR take link stability into account, the energy consumption caused by retransmission can be reduced. The proposed protocol has a lower average energy consumption than the other four routing protocols in a scenario with a speed greater than 20m/s.

Fig. 20 shows the effects of different CBR data rates on AEC. As the data rate increases, the AEC of all protocols increases. When the data rate is higher than 16Kbps, the AEC of TA-AOMDV, QMR and LRMR starts to be lower than QoS-AOMDV and AOMDV. Link stability is considered to be the main reason for the decrease of AEC growth rate when data rate is high. TA-AOMDV not only considers the link stability, but also considers the residual energy of nodes when choosing the path, so its energy efficiency is optimal.

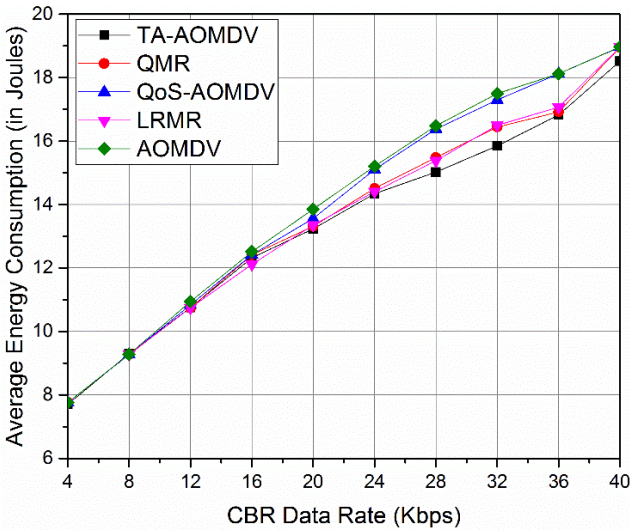

FIGURE 20. Average energy consumption against CBR data rate.

Fig. 21 depicts the AEC of five routing protocols with different number of nodes. When the number of nodes is less than 40, the AEC of the five routing protocols is very close. However, in the range of 40 to 100 nodes, the AEC of TA-AOMDV is higher than that of QMR and QoS-AOMDV. The reason is that LASN packets with abnormal link state feedback consume more energy.

6) DISCUSSION

By comparing the three scenarios, it can be seen that the routing overhead decreases with the increase of CBR data rate and number of nodes, and increases with the increase of node speed. This indicates that speed has an adverse effect on routing overhead.

In order to better compare the network performance of several routing protocols in different speed scenarios, the throughput and routing overhead of the four protocols are

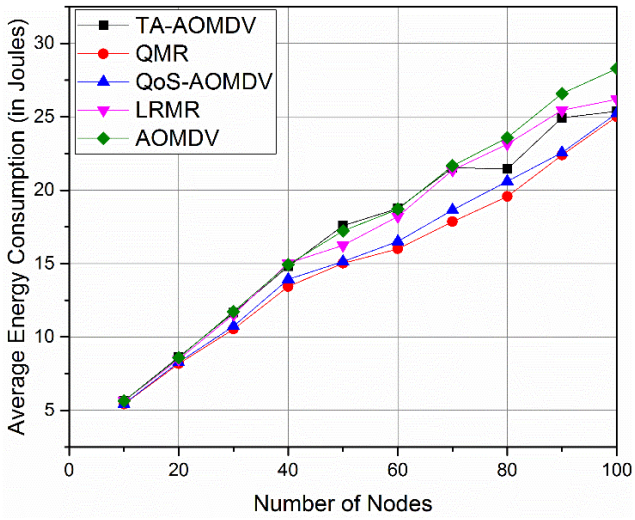

FIGURE 21. Average energy consumption against CBR data rate.

TABLE 2. Throughput versus routing overhead at different speeds.

	TA-AOMDV		QMR		QoS-AOMDV		LRMR	
S	TH	OH	TH	OH	TH	OH	TH	OH
10	36.9	-5.5	19.7	-6.7	10.5	-2.8	5.26	-0.8
20	34.7	43.2	19.7	-8.4	10.5	-2.2	17.1	-0.4
30	27.3	155	19.8	-3.4	10.5	-3.4	18.6	-0.2
40	19.3	203	19.8	-6.7	10.6	-1.2	5.27	-0.18
50	33.9	147	19.8	-4.5	10.6	-1.9	5.28	-0.12

S = node speed (m/s), TH = increment of throughput (%), OH = increment of routing overhead (%).

compared with that of AOMDV, as shown in Table 2.

$$\mathrm{TH} = \frac{Throughput_{(protocol)} - Throughput_{(AOMDV)}}{Throughput_{(AOMDV)}} * 100\% \tag{29}$$

$$\mathrm{OH} = \frac{Overhead_{(protocol)} - Overhead_{(AOMDV)}}{Overhead_{(AOMDV)}} * 100\% \tag{30}$$

where TH is the throughput increment and OH is the increment of routing overhead, which can be obtained from equations (29) and (30) respectively. It can be seen from the data in the table that the throughput of the four protocols is better than AOMDV, in which the TH of QMR and QoS-AOMDV do not change significantly in different speed scenarios. LRMR reaches the maximum increment of 18.6% at the speed of 30m/s, and TA-AOMDV reaches 33.9% at 50m/s. Therefore, in a MANET that allows certain routing overhead, the proposed routing protocol can provide better QoS.

V. CONCLUSION

QoS routing protocols that can adapt to rapid topology changes will help network applications in high-speed MANET, such as Vehicular Ad-hoc network (VANET). In this paper, we propose a new on-demand multipath routing protocol (TA-AOMDV) which can ensure the data transfer on a stable path to some extent. The performance of the proposed protocol is compared with QMR, LRMR, QoS-AOMDV and AOMDV by using NS2. Simulation results in different scenarios (node speed, data rate and number of nodes) show that the proposed TA-AOMDV protocol is superior to the other four protocols in terms of packet delivery ratio, end-to-end delay and throughput. In the high-speed scene with node movement over 25m/s, compared with QMR, LRMR and QoS-AOMDV, TA-AOMDV's PDR was 5.97%, 10.7% and 7.79% higher, E2ED was 48.9%, 53.05% and 51.5% lower, and throughput was 13.1%, 9.28% and 22.5% higher, respectively.

As a future work, the author will explore further to develop routing protocols for high-speed scenarios, which consider both path stability and node density. To adapt to high-speed scenarios, the authors will also attempt to develop a heuristic routing algorithm that allows nodes to infer topology changes based on parameter changes.

ACKNOWLEDGMENT

The authors wish to thank the anonymous referees for their thorough and constructive review of an earlier version of this article.

REFERENCES

[1] M. Younis, "Internet of everything and everybody: Architecture and service virtualization," *Comput. Commun.*, vol. 131, pp. 66–72, Oct. 2018.
[2] H. Zhou, V. C. M. Leung, C. Zhu, S. Xu, and J. Fan, "Predicting temporal social contact patterns for data forwarding in opportunistic mobile networks," *IEEE Trans. Veh. Technol.*, vol. 66, no. 11, pp. 10372–10383, Nov. 2017.
[3] H. Zhou, X. Chen, S. He, J. Chen, and J. Wu, "DRAIM: A novel delayconstraint and reverse auction-based incentive mechanism for WiFi offloading," *IEEE J. Sel. Areas Commun.*, to be published.
[4] G. A. Walikar and R. C. Biradar, "A survey on hybrid routing mechanisms in mobile ad hoc networks," *J. Netw. Comput. Appl.*, vol. 77, pp. 48–63, Jan. 2017, doi: 10.1016/j.jnca.2016.10.014.
[5] W. A. Jabbar, M. Ismail, and R. Nordin, "Energy and mobility conscious multipath routing scheme for route stability and load balancing in MANETs," *Simul. Model. Pract. Theory*, vol. 77, pp. 245–271, Sep. 2017.
[6] W. A. Jabbar, M. Ismail, R. Nordin, and S. Arif, "Power-efficient routing schemes for MANETs: A survey and open issues," *Wireless Netw.*, vol. 23, no. 6, pp. 1917–1952, Aug. 2017.
[7] M. B. Channappagoudar and P. Venkataram, "Performance evaluation of mobile agent based resource management protocol for MANETs," *Ad Hoc Netw.*, vol. 36, pp. 308–320, Jan. 2016.
[8] V. R. Kavitha and M. Moorthi, "A quality of service load balanced connected dominating set-stochastic diffusion search (CDS-SDS) network backbone for MANET," *Comput. Netw.*, vol. 151, pp. 124–131, Mar. 2019.
[9] H. A. Ali, M. F. Areed, and D. I. Elewely, "An on-demand power and load-aware multi-path node-disjoint source routing scheme implementation using NS-2 for mobile ad-hoc networks," *Simul. Model. Pract. Theory*, vol. 80, pp. 50–65, Jan. 2018.
[10] Y. H. Robinson, E. G. Julie, K. Saravanan, L. H. Son, R. Kumar, M. Abdel-Basset, and P. H. Thong, "Link-disjoint multipath routing for network traffic overload handling in mobile ad-hoc networks," *IEEE Access*, vol. 7, pp. 143312–143323, 2019, doi: 10.1109/ACCESS.2019.2943145.
[11] M. Sedrati and A. Benyahia, "Multipath routing to improve quality of service for video streaming over mobile ad hoc networks," *Wireless Pers. Commun.*, vol. 99, pp. 999–1013, Mar. 2018.
[12] S. Hamrioui and P. Lorenz, "EQ-AODV: Energy and QoS supported AODV for better performance in WMSNs," in *Proc. IEEE Int. Conf. Commun. (ICC)*, May 2016, pp. 435–440.

[13] M. Aguilar Igartua and V. Carrascal Frías, "Self-configured multipath routing using path lifetime for video-streaming services over ad hoc networks," *Comput. Commun.*, vol. 33, no. 15, pp. 1879–1891, Sep. 2010.

[14] J. Chen, Z. Li, J. Liu, and Y. Kuo, "QoS multipath routing protocol based on cross layer design for ad hoc networks," in *Proc. Int. Conf. Internet Comput. Inf. Services*, vol. 4, Sep. 2011, pp. 162–165.

[15] M. K. Marina and S. R. Das, "On-demand multipath distance vector routing in ad hoc networks," in *Proc. 9th Int. Conf. Netw. Protocols. (ICNP)*, Nov. 2001, pp. 14–23.

[16] P. Periyasamy and E. Karthikeyan, "Link reliable multipath routing protocol for mobile ad hoc networks," in *Proc. Int. Conf. Circuits, Power Comput. Technol. (ICCPCT)*, Mar. 2015, pp. 1–7.

[17] P. Periyasamy and E. Karthikeyan, "End-to-end link reliable energy efficient multipath routing for mobile ad hoc networks," *Wireless Pers. Commun.*, vol. 92, no. 3, pp. 825–841, 2017.

[18] S. E. Benatia, O. Smail, M. Boudjelal, and B. Cousin, "ESMRsc: Energy aware and stable multipath routing protocol for ad hoc networks in smart city," in *Proc. Int. Conf. Artif. Intell. Renew. Energetic Syst.* Cham, Switzerland: Springer, 2018, pp. 31–42.

[19] F. Rump, S. A. Jopen, and M. Frank, "Using probabilistic multipath routing to improve route stability in MANETs," in *Proc. IEEE 41st Conf. Local Comput. Netw. (LCN)*, Nov. 2016, pp. 192–195, doi: 10.1109/Lcn.2016.40.

[20] S. H. Liu, W. Zeng, Y. Lou, and J. Zhai, "A reliable multi-path routing approach for medical wireless sensor networks," in *Proc. Int. Conf. Identificat., Inf., Knowl. Internet Things (IIKI)*, Oct. 2015, pp. 126–129, doi: 10.1109/Iiki.2015.35.

[21] R. D. Gomes, D. V. Queiroz, A. C. Lima Filho, I. E. Fonseca, and M. S. Alencar, "Real-time link quality estimation for industrial wireless sensor networks using dedicated nodes," *Ad Hoc Netw.*, vol. 59, pp. 116–133, May 2017.

[22] N. Sofra, A. Gkelias, and K. K. Leung, "Route construction for long lifetime in VANETs," *IEEE Trans. Veh. Technol.*, vol. 60, no. 7, pp. 3450–3461, Sep. 2011.

[23] M. Ghafouri Vaighan and M. A. Jabraeil Jamali, "A multipath QoS multicast routing protocol based on link stability and route reliability in mobile ad-hoc networks," *J. Ambient Intell. Humanized Comput.*, vol. 10, no. 1, pp. 107–123, Jan. 2019.

[24] A. P. Reddy and N. Satyanarayana, "Energy-efficient stable multipath routing in MANET," *Wireless Netw.*, vol. 23, no. 7, pp. 2083–2091, Oct. 2017.

[25] S.-S. Wang and Y.-S. Lin, "PassCAR: A passive clustering aided routing protocol for vehicular ad hoc networks," *Comput. Commun.*, vol. 36, no. 2, pp. 170–179, Jan. 2013.

[26] M. A. Gawas, K. Modi, P. Hurkat, and L. J. Gudino, "QoS based multipath routing in MANET: A cross layer approach," in *Proc. Int. Conf. Commun. Signal Process. (ICCSP)*, Apr. 2017, pp. 1806–1812.

[27] D. Chander and R. Kumar, "QoS enabled cross-layer multicast routing over mobile ad hoc networks," *Procedia Comput. Sci.*, vol. 125, pp. 215–227, 2018, doi: 10.1016/j.procs.2017.12.030.

[28] G. Singal, V. Laxmi, M. S. Gaur, S. Todi, V. Rao, M. Tripathi, and R. Kushwaha, "Multi-constraints link stable multicast routing protocol in MANETs," *Ad Hoc Netw.*, vol. 63, pp. 115–128, Aug. 2017.

[29] F. Abbas and P. Fan, "Clustering-based reliable low-latency routing scheme using ACO method for vehicular networks," *Veh. Commun.*, vol. 12, pp. 66–74, Apr. 2018, doi: 10.1016/j.vehcom.2018.02.004.

[30] D. K. Lobiyal, C. P. Katti, and A. K. Giri, "Parameter value optimization of ad-hoc on demand multipath distance vector routing using particle swarm optimization," *Procedia Comput. Sci.*, vol. 46, pp. 151–158, Jan. 2015, doi: 10.1016/j.procs.2015.02.006.

[31] A. K. Giri, D. K. Lobiyal, and C. P. Katti, "Optimization of value of parameters in ad-hoc on demand multipath distance vector routing using teaching-learning based optimization," *Procedia Comput. Sci.*, vol. 57, pp. 1332–1341, Jan. 2015, doi: 10.1016/j.procs.2015.07.445.

[32] A. Naushad, G. Abbas, Z. H. Abbas, and A. Pagourtzis, "Novel strategies for path stability estimation under topology change using hello messaging in MANETs," *Ad Hoc Netw.*, vol. 87, pp. 76–99, May 2019.

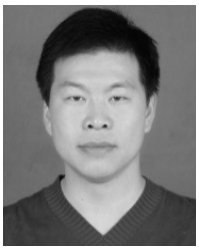

ZHENG CHEN received the master's degree in communication and information system from the Nanchang University, China, in 2009. He is currently pursuing the Ph.D. degree with the School of Optical and Electronic Information, Huazhong University of Science and Technology, China. His current research interests include modeling and simulation of mobile wireless ad hoc networks (MANets), wireless sensor networks, and the IoT.

WENLI ZHOU (Member, IEEE) received the bachelor's degree in measurement technology and instrumentation, and the master's degree in semiconductor devices and microelectronics from the Huazhong University of Science and Technology (HUST), China, in 1990 and 1995, respectively, and the Ph.D. degree, in 2004. She joined as a Faculty Member with the Department of Electronic Science and Technology, HUST, in 1995, where she is involved in the teaching and research of microelectronics. From 2000 to 2005, she was a Ph.D. Student and a Postdoctoral Fellow with the Department of Automation and Computer-Aided Engineering, the Chinese University of Hong Kong. She was a Visiting Scholar with the Department of Mechanical and Aerospace Engineering, UCLA, from 2014 to 2015. She is currently a Professor with the School of Optical and Electronic Information, HUST. She is the author of one book chapter, over 60 articles, and over 20 authorized patents. Her current research interests are the interface technology of novel merged networks, and implementation by using FPGA and embedded systems.

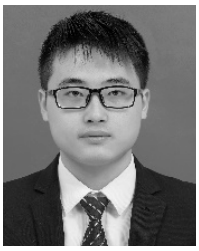

SHUO WU received the bachelor's degree in measuring and control technology and instruments from the North China University of Water Resources and Electric Power, China, in 2018. He is currently pursuing the master's degree with the School of Optical and Electronic Information, Huazhong University of Science and Technology, China. His research interests are neuromorphic device and neural networks.

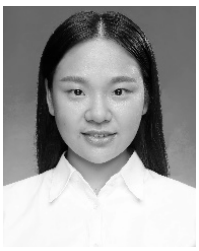

LI CHENG received the bachelor's degree in optoelectronic information science and engineering from the China University of Mining and Technology, China, in 2018. She is currently pursuing the master's degree with the School of Optical and Electronic Information, Huazhong University of Science and Technology, China. Her research interest is wireless sensor networks.